Journal of Controlled Release 304 (2019) 29–38

Contents lists available at ScienceDirect

Journal of Controlled Release

journal homepage: www.elsevier.com/locate/jconrel

Dexmedetomidine enhances glymphatic brain delivery of intrathecally administered drugs

Tuomas O. Lilius[a,b,c,d,*], Kim Blomqvist[b,d], Natalie L. Hauglund[a], Guojun Liu[e], Frederik Filip Stæger[a], Simone Bærentzen[a], Ting Du[e], Fredrik Ahlström[b,d], Janne T. Backman[c,d], Eija A. Kalso[b,f], Pekka V. Rauhala[b,d], Maiken Nedergaard[a,e]

[a] Center for Translational Neuromedicine, Faculty of Health and Medical Sciences, University of Copenhagen, Copenhagen, Denmark
[b] Department of Pharmacology, Faculty of Medicine, University of Helsinki, Helsinki, Finland
[c] Department of Clinical Pharmacology, Faculty of Medicine, University of Helsinki, Helsinki University Hospital, Helsinki, Finland
[d] Individualized Drug Therapy Research Program, Faculty of Medicine, University of Helsinki, Helsinki, Finland
[e] Center for Translational Neuromedicine, University of Rochester Medical Center, Rochester, NY, USA
[f] Department of Anaesthesiology, Intensive Care Medicine, and Pain Medicine, Helsinki University Hospital, University of Helsinki, Finland

ARTICLE INFO

Keywords:
Drug delivery
Glymphatic system
Pharmacokinetics
α_2-adrenergic agonist
Dexmedetomidine
Opioid
Amyloid-β
Antibody therapy

ABSTRACT

Drug delivery to the central nervous system remains a major problem due to biological barriers. The blood-brain-barrier can be bypassed by administering drugs intrathecally directly to the cerebrospinal fluid (CSF). The glymphatic system, a network of perivascular spaces promoting fluid exchange between CSF and interstitial space, could be utilized to enhance convective drug delivery from the CSF to the parenchyma. Glymphatic flow is highest during sleep and anesthesia regimens that induce a slow-wave sleep-like state. Here, using mass spectrometry and fluorescent imaging techniques, we show that the clinically used α_2-adrenergic agonist dexmedetomidine that enhances EEG slow-wave activity, increases brain and spinal cord drug exposure of intrathecally administered drugs in mice and rats. Using oxycodone, naloxone, and an IgG-sized antibody as relevant model drugs we demonstrate that modulation of glymphatic flow has a distinct impact on the distribution of intrathecally administered therapeutics. These findings can be exploited in the clinic to improve the efficacy and safety of intrathecally administered therapeutics.

1. Introduction

Drug delivery to the central nervous system (CNS) is particularly difficult due to the blood-brain barrier (BBB). Direct administration to the cerebrospinal fluid (CSF) is used to bypass the BBB to deliver several classes of small-molecule drugs, including local anesthetics, analgesics, antibiotics, and chemotherapy agents, as well as larger therapeutics such as polypeptides [1], proteins [2], or oligonucleotides. For example, the intrathecally administered oligonucleotide nusinersen is currently the only disease-modifying treatment for spinal muscular atrophy [3]. However, the slow diffusion rate of solutes from the CSF to the CNS interstitial fluid (ISF) has been thought to severely restrict the entry of intrathecally administered therapeutics to the deeper regions of the brain and spinal cord [4].

The recently discovered glymphatic pathway is a fluid transport system that facilitates the influx of CSF to the CNS interstitium. [5,6] CSF in the subarachnoid space flows along the periarterial spaces of large leptomeningeal arteries [6,7]. After branch points of the arterial vasculature, CSF flows to deeper brain and spinal cord structures alongside the periarterial (Virchow-Robin) spaces of penetrating arteries [6,8]. Astrocytic endfeet that face the periarterial spaces express highly polarized aquaporin 4 (AQP4) water channels that facilitate CSF influx from the periarterial spaces into the interstitial space [9]. This CSF-ISF exchange process facilitates a net fluid movement in the brain interstitium towards venous perivascular sites, which in turn drain to arachnoid granulations, cranial and spinal nerves, as well as meningeal lymphatic vessels [10,11]. Glymphatic fluxes effectively clear the brain of many endogenous macromolecules, such as amyloid-β [6] and tau [12] and small-molecular weight metabolites, such as lactate [13]. In addition to clearance, glymphatic flow has also been shown to distribute fluorescent tracers of different sizes from the CSF into the brain [6,7] and the spinal cord [14].

The glymphatic pathway is predominantly active during sleep [15] or anesthesia that promotes slow-wave oscillations [15,16]. Decreased

* Corresponding author at: Center for Translational Neuromedicine, University of Copenhagen, Blegdamsvej 3B, 2200 Copenhagen N, Denmark.
E-mail address: tuomas.lilius@sund.ku.dk (T.O. Lilius).

https://doi.org/10.1016/j.jconrel.2019.05.005
Received 12 March 2019; Received in revised form 28 April 2019; Accepted 3 May 2019
Available online 05 May 2019

CNS noradrenergic tone, an important feature of deep NREM sleep, has been associated with high glymphatic influx as it decreases resistance to interstitial fluid flow by enlarging the interstitial space volume [15]. Dexmedetomidine, a selective α_2-adrenergic agonist, is a sedative agent commonly used in intensive care and procedural sedation [17,18]. It induces a sedative state similar to stage II–III NREM sleep with respect to the increased slow-wave delta oscillations in the electroencephalogram (EEG) and dramatically decreased noradrenergic tone [19]. So far, it remains largely uncharacterized whether pharmacologic modulation of glymphatic flow by dexmedetomidine or other drugs could affect the CNS pharmacokinetics of drugs administered either intrathecally or systemically.

In clinical practice, intrathecal drugs are usually administered during the awake state when the glymphatic system is disengaged. We hypothesized that enhancing glymphatic CSF influx by either systemic or intrathecal dexmedetomidine should increase the delivery of intrathecally administered drugs from the CSF to the interstitium. We studied the glymphatic CNS delivery of clinically relevant small-molecule drugs as well as an IgG-sized therapeutic. We found that in several brain areas critical for opioid analgesia and toxicity the availability of intrathecally administered oxycodone and naloxone were markedly increased by subcutaneous or intrathecal dexmedetomidine co-administration. We propose that the modulation of the glymphatic system by α_2-adrenergic agonists could be potentially used clinically to enhance the CNS delivery of certain intrathecally administered drugs.

2. Materials and methods

2.1. Animals

All procedures were approved by the local authorities (Regional State Administrative Agency of Southern Finland, ESAVI/9697/04.10.07/2017, Animal Experiments Council under the Danish Ministry of Environment and Food, 2015-15-0201-00535, and University Committee on Animal Resources of the University of Rochester Medical Center, 2011-023). Male Sprague-Dawley rats (200–250 g, Harlan, Horst, The Netherlands and 300–350 g, Charles River, Salzburg, Germany in experiments assessing physiological function) and adult male C57BL/6 mice (23–26 g, Charles River, Wilmington, MA, USA) were used. They were housed in individually ventilated plastic cages in light- and temperature-controlled rooms. Water and standard laboratory pellets were available ad libitum. After the placement of cisterna magna cannulas, animals were single-housed for one day.

2.2. Drugs

Buprenorphine hydrochloride (Temgesic®, 0.3 mg/mL, Indivior, Slough, UK), carprofen (Rimadyl® vet, 50 mg/mL, Pfizer, Espoo, Finland), dexmedetomidine hydrochloride (Dexdomitor®, 0.5 mg/mL, Orion Pharma, Espoo, Finland), lidocaine hydrochloride (Lidocain®, 20 mg/mL, Orion Pharma), and morphine hydrochloride powder were purchased from the University Pharmacy (Helsinki, Finland). Oxycodone hydrochloride powder and naloxone hydrochloride powder were purchased from Sigma-Aldrich (St. Louis, MO, USA). Buprenorphine, carprofen, and dexmedetomidine were diluted in physiological saline and administered subcutaneously in a volume of 2 mL/kg. Lidocaine was diluted to 5 mg/mL and used for local infiltration anesthesia. For intrathecal injections, morphine, naloxone, and oxycodone were diluted in sterile physiological saline.

2.3. Intracisternal cannulations and drug infusions

The cisterna magna cannulation procedure was performed as previously described with minor modifications [20]. In mice, intracisternal cannulas were placed under ketamine-xylazine anesthesia. In rats, isoflurane 3% anesthesia was used. After verification of loss of response to toe pinch, animals were placed in a stereotaxic frame with the neck slightly flexed (30–40°). The atlanto-occipital membrane overlying the cisterna magna was exposed and a 30G needle connected to a 4-cm long PE10 tubing was carefully inserted into the intrathecal space. The catheter was fixed to the dura with cyanoacrylate glue and dental cement. Animals were monitored post-operatively and normothermia was maintained with a heating pad. For post-operative analgesia, rats received s.c. carprofen (5 mg/kg) and buprenorphine (0.05 mg/kg) at the beginning of surgery.

On the morning of the next day after the cannulations, rats were randomly allocated to either the awake group (saline) or the sedation group (0.2 mg/kg dexmedetomidine s.c.). Ten minutes after the injection, awake rats were gently guided into a restrainer on a heating pad. Dexmedetomidine-sedated rats had lost the righting reflex by 10 min and were transferred to the heating pad and placed prone on it. Oxycodone (100 nmol) and naloxone (100 nmol) or morphine (100 nmol) and naloxone (100 nmol) were co-infused into the rat cisterna magna using a KD Scientific Legato® 130 pump (Holliston, MA, USA) attached to a Hamilton Gastight 1700 microsyringe (Bonaduz, Switzerland). The infusion rate of 1.6 μL/min was chosen based on previous findings showing no effect on intracranial pressure with this infusion rate (41). The total volume of 20 μL was infused over 12.5 min, with a total effective volume of 16 μL. After the infusion, animals in the awake groups were kept awake by non-aversive sleep deprivation (introduction of new object for exploration and gentle brushing), whereas the dexmedetomidine-sedated rats were placed prone on a heating pad in a quiet environment and kept normothermic. Depending on the experiment, rats were killed by decapitation for collection of blood, brain and spinal cord samples at 30, 60, or 120 min after the beginning of the infusion. The effects of dexmedetomidine on drug distribution in other organs was not studied. All samples were collected and analyzed by investigators blinded to the treatment groups.

To study amyloid-β antibody distribution, mice were either awake or sedated with 0.018 or 0.2 mg/kg i.p. dexmedetomidine. After 10 min, they were intracisternally infused 2% Alexa Fluor 488-conjugated anti-β-amyloid 1–16 antibody (clone 6E10, 1 mg/mL; BioLegend, catalog 803013) in artificial CSF over 5 min using an infusion rate of 2 μL/min (7). After a distribution period of 60 min and euthanasia by decapitation, brains were removed and drop-fixed in 4% paraformaldehyde for 24 h.

2.4. EEG electrode implantation and EEG recordings

Rats were anesthetized with 2–3% isoflurane, and the head was fixed in a stereotactic frame. Four holes (0.8 mm) were drilled in the skull bilaterally above the parietal and frontal cortex by using bregma, lambda, and the midline as reference points. Great care was taken not to damage the underlying dura. Two 0.8 mm stainless steel screws (NeuroTek, Wheat Ridge, CO, USA) were attached in the left hemisphere holes to serve as anchors, and two low impedance stainless steel screws (NeuroTek) were attached to the right hemisphere holes. After implantation of all four bone screws, a thin layer of dental glue was applied to cover the screws and allowed to dry, followed by application of a layer of dental cement on top of the glue. The rats recovered in controlled temperature and received s.c. carprofen (5 mg/kg) post-operatively and after 24 and 48 h.

For the EEG recordings, a shielded cable was connected to the recording electrodes and to a preamplifier (Molecular Devices, San Jose, CA, USA). Signals were digitized at a sampling rate of 500 Hz and collected with Clampex software (Molecular Devices). The rat freely moved around in a container while obtaining the baseline awake EEG. After administration of dexmedetomidine or vehicle, EEG was recorded continuously for the following 120 min. For analysis, the recording was divided into 5-min epochs and an artifact-free epoch from the awake recording session was used as the baseline. EEG traces were analyzed with Matlab (Mathworks, Natick, MA, USA). The EEG power was

calculated for the delta (0.5–4 Hz), theta (4–8 Hz), and alpha frequencies (8–12 Hz) by fast Fourier transform, and the percentage of power in each frequency range was calculated from the total power of the 0–50 Hz spectrum.

2.5. Physiological measurements

Systolic and diastolic blood pressure and heart rate were assessed with a non-invasive rat CODA Surgical Monitor (Kent Scientific, Torrington, CT, USA). Respiratory rate was assessed by visual calculation over a 60-s period.

2.6. Small-molecule drug concentration measurements

Rats were decapitated and trunk blood was collected in K2-EDTA tubes. Plasma was separated by centrifugation at 2000*g* for 10 min at +4 °C and stored at −80 °C. Brain (dorsal cortex, ventral cortex, dorsal hippocampus, thalamus, hypothalamus) and spinal cord (lumbar enlargement area) samples were carefully dissected, weighed, rinsed in phosphate-buffered saline, snap-frozen in liquid nitrogen, and stored at −80 °C before analysis. Tissue samples were homogenized and diluted in 0.5–1 mL of sterile water. The determination of morphine, naloxone, and oxycodone was performed as described previously [21] with minor modifications using SHIMADZU UHPLC Nexera X2 liquid chromatography system (SHIMADZU USA Manufacturing Inc. Canby, OR, USA) coupled to an API 3000 tandem mass spectrometer (AB Sciex, Toronto, Ontario, Canada) operating in a positive turbo ion spray mode. The chromatographic separations were achieved on Atlantis HILIC Silica column (3 µm particle size, 2.1 × 100 mm I.D.; Waters, Milford, MA, USA) using a gradient elution of mobile phase consisting of acetonitrile and 20 mmol/L ammonium formate in 0.2% formic acid (v/v). An aliquot (10 µL) was injected at a flow rate of 200 µL/min to give a total chromatographic run time of 22 min. Deuterium-labelled standards were used for morphine, oxycodone (Cerilliant, Round Rock, TX, USA), and naloxone (Sigma-Aldrich). The target ion transitions monitored were as follows: morphine *m/z* 286 → 152, naloxone m/z 328 → 253, and oxycodone m/z 316 → 241. The limits of quantification (LOQ) were 3.5 pmol/mL morphine, 3.1 pmol/mL naloxone, and 0.79 pmol/mL oxycodone. The calibration curves were linear over the concentration range of LOQ–250 ng/mL, and day-to-day coefficients of variation were below 15% within the relevant concentration range for all analytes. None of the measured compounds interfered with the mass spectrometric assay.

2.7. Fluorescent antibody concentration analyses

Dorsal and ventral whole brain images were acquired on stereomicroscope (MVX10, Olympus, Tokyo, Japan). Exposure times and magnifications were kept the same for all groups. To allow qualitative visual comparison of the effects of different doses of dexmedetomidine on CSF tracer influx, a population-based average combining the images from all groups was created for both the ventral and dorsal macroscopic images. First, an initial average template was computed as the mean of the nonaligned images. Then, all images were registered to this average template, and a new mean of the aligned images was computed. Registering and averaging were repeated with increasingly refined registration methods (three iterations of rigid registration, followed by two affine registration iterations and lastly by three nonlinear registration iterations), resulting in the final population-based average template. Last, all images were nonlinearly registered to the appropriate template to allow group comparisons. Image registration was performed using Advanced Normalization Tools (ANTs) 2.1.0 [22] and scripted with Python 3.6.

2.8. Statistical analysis

The data are presented as means ± SD. Two-tailed *t*-tests for repeated measurements with Holm-Sidak correction or analyses of variance (ANOVA) followed by Holm-Sidak post hoc analysis were performed. Statistical significance was ascribed at $P < .05$. The data were analyzed using GraphPad Prism, version 7.0c for Mac OS X (GraphPad Software, La Jolla, CA).

3. Results

3.1. Dexmedetomidine increases the brain delivery of an IgG-sized antibody therapeutic

Using a method that has been previously validated for studying glymphatic drug delivery [7], we first assessed whether dexmedetomidine could increase the brain delivery of an amyloid-ß antibody, an example of an IgG-sized (~150 kDa) biological drug with no known active transport at the BBB. Mice that had received cisterna magna cannulas 24 h earlier received either dexmedetomidine or vehicle and 10 min later a cisterna magna infusion of Alexa Fluor 488-conjugated fluorescent amyloid-β antibody (Fig. 1A). After a distribution time of 60 min, the brains were extracted, fixed, and analyzed for fluorescence from both the dorsal and ventral sides (Fig. 1B–C). Because the measurable penetration of IgG-sized drugs to deep brain structures is very low, instead of using a standard coronal slice technique we used a macroscopic technique that enables imaging of the entire ventral and dorsal brain surfaces to a penetration depth of up to 1–2 mm [7]. Glymphatic CSF influx assessed by macroscopic imaging highly correlates with coronal slice analyses [16]. We found that whereas the low dexmedetomidine (0.018 mg/kg i.p.) dose did not have an effect compared with vehicle, the high-dose dexmedetomidine treatment (0.2 mg/kg i.p.) approximately doubled the amyloid-ß antibody delivery to both the dorsal and the ventral brain surfaces (Fig. 1D).

3.2. Effects of dexmedetomidine on physiological function

Having confirmed that dexmedetomidine increases the brain availability of an IgG-sized therapeutic, we continued the small-molecule drug experiments in rats because of more tissue available for quantitative mass spectrometry analyses in homogenized samples. We chose the positive dose (0.2 mg/kg) from the previous experiment and characterized its effects on physiological parameters in rats after s.c. administration (Fig. 2A). Dexmedetomidine caused a significant increase in EEG delta power during the whole 120-min measurement period (Fig. 2B), with a concomitant minor and non-significant decrease in the alpha and theta powers. The blood pressure increased immediately following dexmedetomidine administration and gradually decreased to baseline levels thereafter (Fig. 2C), whereas heart rate and respiratory rate were unaffected (Fig. 2D).

3.3. Systemic dexmedetomidine sedation enhances CNS delivery of intrathecally administered oxycodone and naloxone

We then infused morphine together with the opioid antagonist naloxone to the cisterna magna of groups of awake (i.e. vehicle-treated) or dexmedetomidine-sedated rats (Fig. 3A). We chose morphine as the first intrathecally administered opioid, as it is frequently administered in neuraxial anesthesia. Naloxone was co-infused with morphine to avoid respiratory depression, opioid-induced sedation, and other potential adverse effects of morphine. To identify the times of maximum concentration (T_{max}) in the brain, we collected tissue and plasma samples at 30, 60, and 120 min after the start of the 12.5-min drug infusion. Concentrations of both drugs were simultaneously determined using high-performance mass spectrometry-tandem liquid chromatography. Despite similar molar doses (100 nmol) of infused morphine and

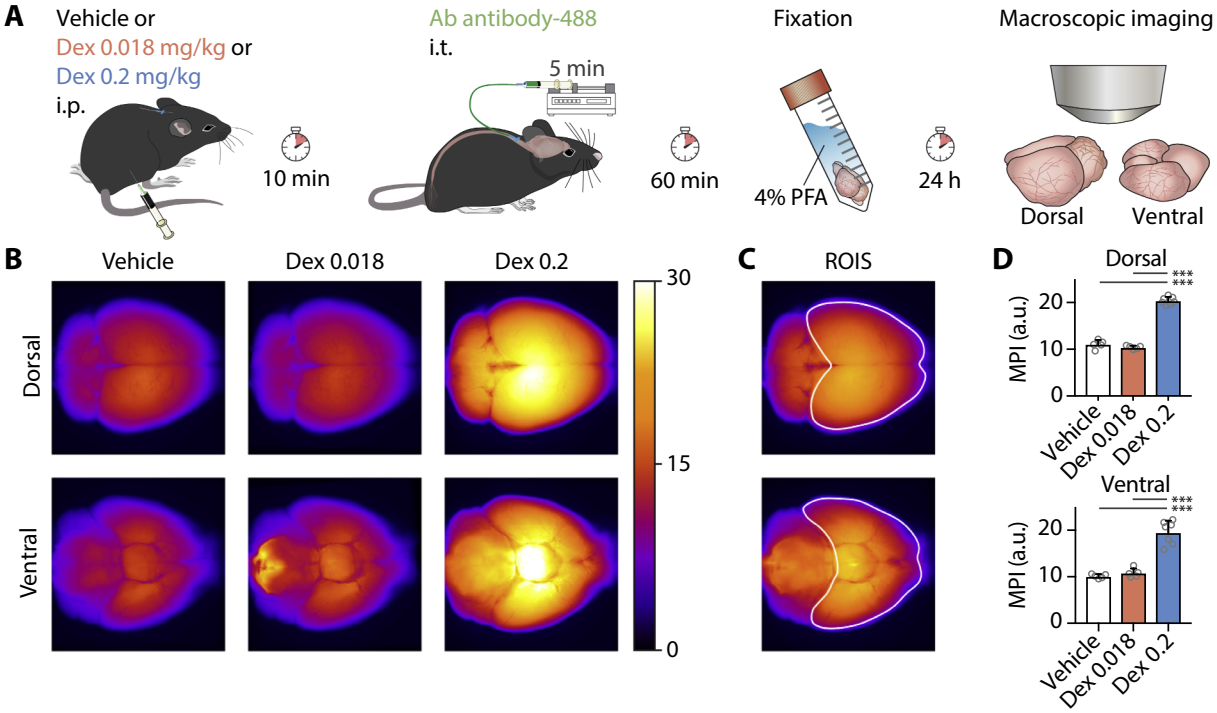

Fig. 1. Dexmedetomidine increases the distribution of intrathecally-infused fluorescent amyloid-β antibody to the brain ventral and dorsal surfaces as assessed by a fluorescent macroscopic technique. (A) Mice received two doses of dexmedetomidine (Dex, 0.018 mg/kg or 0.2 mg/kg i.p.) or vehicle and 10 min later an intracisternal infusion of a fluorescent amyloid-β antibody-488. After 60 min of circulation, mice were killed and the brains fixed with paraformaldehyde (PFA) for 24 h. (B) Population-based average of amyloid-β antibody distribution at the dorsal and ventral brain surfaces. (C) Regions of interest (ROIS, shown in white) used for the mean pixel intensity (MPI) measurements. (D) Dorsal and ventral region of interest MPI measurements for each brain. Measurements are divided into the vehicle, Dex 0.018, and Dex 0.2 group. Each group is presented as mean (± SD) with the individual data points shown in grey (a.u., arbitrary units). ***$P < .001$ (n = 5–7); one-way ANOVA with Holm-Sidak post-test.

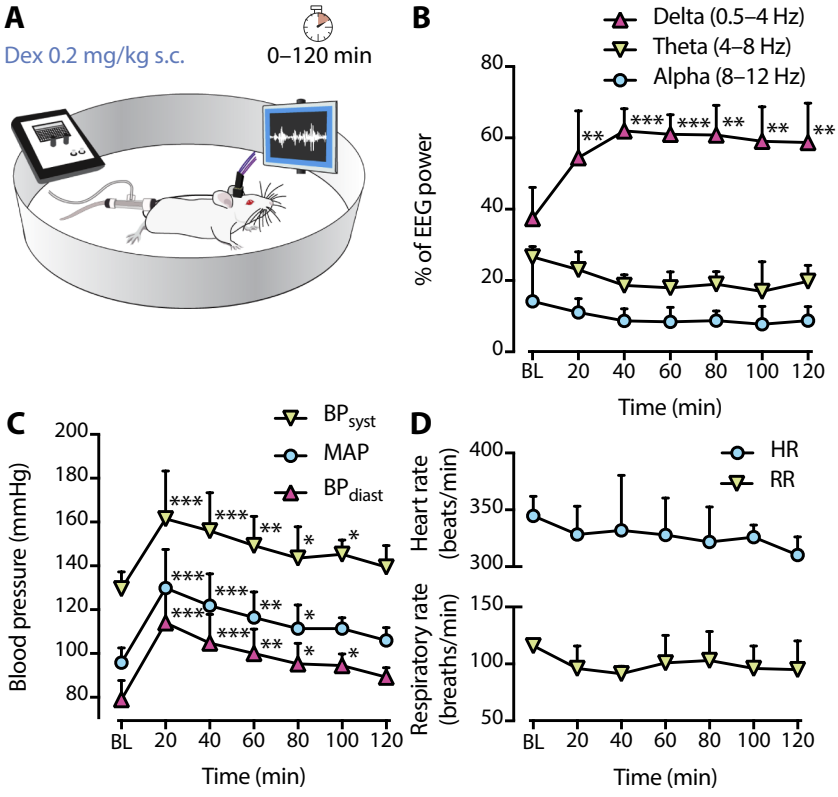

Fig. 2. Dexmedetomidine (0.2 mg/kg, s.c.) induces sedation with enhanced electroencephalogram (EEG) slow-wave delta activity and transient hypertension, but is without effects on respiratory or heart rate. (A) Simultaneous EEG, blood pressure, heart rate, and respiratory rate measurements were performed first awake and then for 120 min under dexmedetomidine sedation. Baseline measurements were conducted immediately before dexmedetomidine administration, prior to onset of action. (B) Compared with wakefulness, dexmedetomidine increased the EEG delta power over the whole measurement period. (C) Compared with wakefulness, dexmedetomidine increased the systolic (BP_{syst}) and distolic (BP_{diast}) blood pressure and mean arterial pressure (MAP) for 100 min. The MAP was calculated from RR_{syst} and RR_{diast} values. (D) Dexmedetomidine did not affect heart rate or respiratory rate during the measurement period. Means (± SD) are presented. ***$P < .001$, **$P < .01$, *$P < .05$ (n = 4); two-way repeated-measures ANOVA with Holm-Sidak post-test.

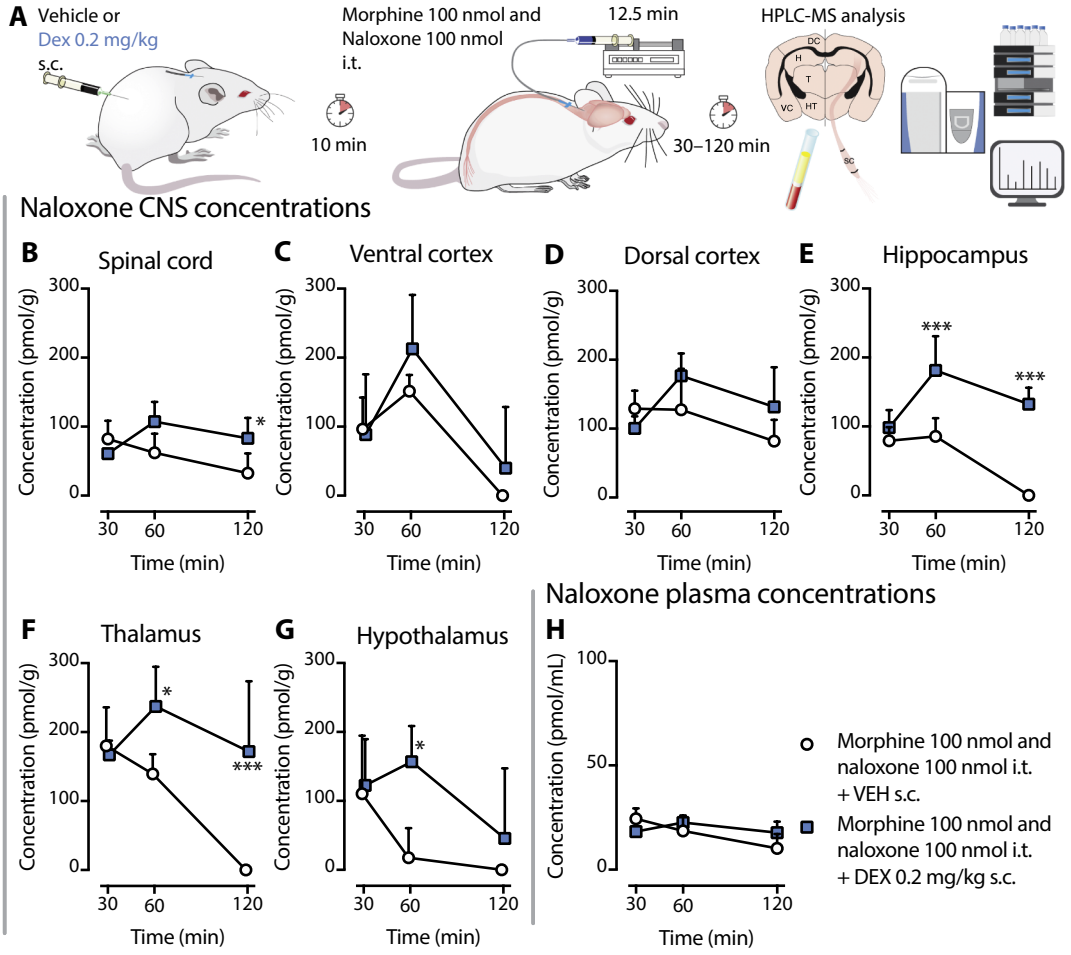

Fig. 3. Dexmedetomidine (Dex) increases the concentrations of intrathecally-infused naloxone in the brain and spinal cord at 60–120 min after infusion. (A) Rats received either vehicle or dexmedetomidine at −10 min and an intracisternal infusion of morphine together with naloxone at 0 min. To assess the time-concentration profiles in the CNS, rats were killed at 30–120 min after the beginning of the infusion, samples of brain regions, the spinal cord lumbar enlargement, and trunk blood were collected. Morphine concentration measurements are not shown due to very low concentrations falling below the limit of quantification. (B–G) Dexmedetomidine sedation increased the total naloxone concentration in the hippocampus, thalamus, and hypothalamus at 60 min and in the spinal cord, hippocampus, and thalamus at 120 min. T_{max}, the time point of maximum naloxone concentration in dexmedetomidine-sedated rats was at 60 min after infusion in all CNS areas. (H) Dexmedetomidine sedation did not affect the plasma concentrations of intrathecally-infused naloxone. Means (± SD) are presented. ***$P < .001$, *$P < .05$ (n = 3–6); two-way ANOVA with Holm-Sidak post-test.

naloxone, the morphine concentrations in the CNS were below the limit of quantification, possibly due to very high drug efflux transport from the CNS. Naloxone concentrations were quantifiable in all CNS regions.

The T_{max} for naloxone in the awake rats occurred already at 30 min in most areas of interest (Fig. 3B–G), with a fast, subsequent concentration decline in the CNS. The dexmedetomidine-sedated rats showed a distinctly different pharmacokinetic profile, with the naloxone T_{max} occurring at 60 min, and attaining markedly increased drug exposure in the hippocampus, thalamus and hypothalamus compared with the vehicle-treated rats. At 120 min after infusions, naloxone concentrations in the dexmedetomidine-sedated rats remained particularly high in the hippocampus and thalamus, clearly exceeding those of the vehicle-treated rats. The plasma naloxone concentrations (Fig. 3H) did not differ between vehicle and dexmedetomidine groups at any observation time point, thus excluding peripheral factors such as decreased systemic clearance.

Because we could not detect morphine concentrations in the CNS, we studied another opioid agonist, oxycodone, that has active influx transport to the brain (20). Oxycodone (100 nmol) was co-infused with 100 nmol naloxone, as above (Fig. 4A). We confined our focus to 60 min post infusion, the T_{max} point found for naloxone in the previous experiment. Compared with vehicle, dexmedetomidine treatment increased concentrations of oxycodone by 24 to 96% in the spinal cord, ventral cortex, dorsal cortex, thalamus, and hypothalamus, with highest concentrations obtained in the dorsal cortex (Fig. 4B). As with findings in the experiments with morphine, the naloxone concentrations were markedly increased in the hippocampus, thalamus, and hypothalamus of the sedated animals, with the highest concentrations in thalamus (Fig. 4C). As dexmedetomidine did not influence the plasma concentrations of oxycodone and naloxone (Fig. 4D), we found increased CNS region-to-plasma concentration ratios for both intrathecally administered drugs (Fig. 4E–F).

3.4. Dexmedetomidine administered as an intrathecal adjuvant increases CNS opioid exposure

In humans, dexmedetomidine is typically administered systemically, however, there are reports for off-label intrathecal use as an adjuvant to other anesthetics and analgesics [34]. We tested the hypothesis that intrathecal dexmedetomidine could be used as an intrathecal adjuvant with other small-molecule drugs to increase their access to the CNS. In the experiment, cisterna magna cannulas were placed acutely under brief isoflurane (3%) anesthesia. Isoflurane was maintained at 1.5% during the infusions and was discontinued afterwards. Rats first

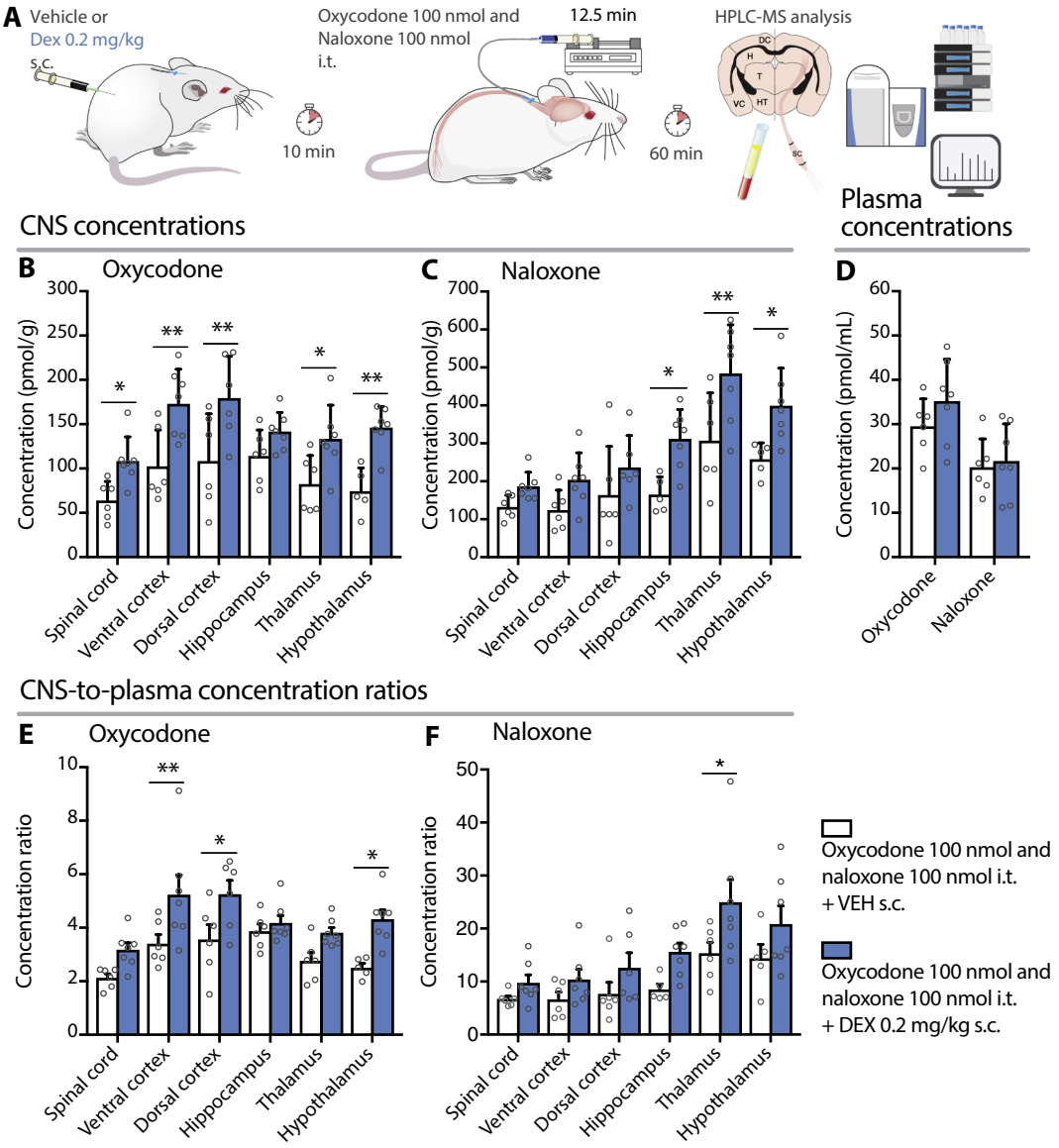

Fig. 4. Dexmedetomidine (Dex) enhances the delivery of intrathecally-administered oxycodone and naloxone to the brain and spinal cord. (A) Rats received either vehicle or dexmedetomidine at −10 min and an intracisternal infusion of oxycodone and naloxone at 0 min. Rats were killed at 60 min, based on results of previous experiment showing the maximum naloxone concentrations (T_{max}) for at 60 min. (B) Dexmedetomidine increased the concentrations of oxycodone at several CNS areas relevant to antinociception, including the spinal cord lumbar enlargement, cortex and thalamus. The greatest increase (96%) was observed in the hypothalamus. (C) In agreement with the previous experiment, dexmedetomidine increased also the naloxone concentrations in the hippocampus, thalamus and hypothalamus at 60 min. (D) Corresponding plasma concentrations of oxycodone and naloxone did not reveal any differences between groups. (E–F) The CNS region-to-plasma concentration ratios for oxycodone and naloxone increased in the treatment group, indicating increased brain availability. Means (± SD) are shown (n = 6–7). $^{**}P < .01$, $^{*}P < .05$; t-test with Holm-Sidak correction for multiple comparisons.

received an intracisternal infusion of either saline or dexmedetomidine (8 μg in 16 μL) directly followed by oxycodone (100 nmol) and naloxone (100 nmol) (Fig. S1A). Samples were collected 60 min after the start of the infusion of oxycodone and naloxone. Intrathecal dexmedetomidine adjuvant increased both the oxycodone (Fig. S1B) and naloxone (Fig. S1C) concentrations in the three studied important locations for opioid analgesia; the spinal cord, thalamus, and dorsal cortex. However, the magnitude of effect was slightly smaller than in the experiments with systemic dexmedetomidine. The greatest increase in oxycodone concentrations by dexmedetomidine was 41% in the spinal cord. The plasma concentrations of oxycodone or naloxone did not differ between groups (Fig. S1D). The CNS-to-plasma concentration ratio of oxycodone (Fig. S1E) was significantly increased in the spinal cord and thalamus by dexmedetomidine, however, for naloxone there was no significant change (Fig. S1F).

Finally, to rule out a potential system-level pharmacokinetic interaction between dexmedetomidine, oxycodone, and naloxone, we administered subcutaneous dexmedetomidine (0.2 mg/kg) or vehicle followed by oxycodone and naloxone (1 mg/kg each, s.c.) (Fig. S2A). Dexmedetomidine did not significantly affect plasma oxycodone or naloxone concentrations at 30 or 60 min after administration or CNS concentration at 60 min after administration (Fig. S2B–E). Consequently, the CNS region-to-plasma concentration ratios of systemically administered oxycodone and naloxone were not changed by dexmedetomidine (Fig. S2F–G).

4. Discussion

We found that both systemic and intrathecal dexmedetomidine substantially increased the delivery of two intrathecally administered

small-molecule drugs, oxycodone and naloxone, to the brain and spinal cord. Systemic dexmedetomidine increased the CNS oxycodone concentration in several CNS areas, ranging from a 24% increase in the hippocampus to a 96% increase in the hypothalamus region. The increases in naloxone concentrations were of similar magnitude. Importantly, the CNS-to-plasma concentration ratios of intrathecally administered oxycodone and naloxone were both increased by dexmedetomidine, predicting greater exposure to the drugs. In systemic co-administration, neither the mean CNS and plasma concentrations nor the corresponding CNS-to-plasma concentration ratios for oxycodone and naloxone were affected, ruling out any significant systemic pharmacokinetic interaction or altered competition for transport at the BBB. In addition to the small-molecule drugs, dexmedetomidine also increased the brain delivery of an intrathecally administered IgG-sized therapeutic as assessed by standard fluorescent methods. We propose that the glymphatic drug delivery pathway evidently activated by dexmedetomidine can be utilized to enhance CNS delivery of therapeutics upon intrathecal administration.

The study shows that pharmacologic activation of the glymphatic pathway can enhance the CNS distribution of drugs of low molecular weight (~300 Da). After intrathecal infusion, we detected significant oxycodone concentrations in brain areas important for its analgesic actions, such as the spinal cord, thalamus, and cortex. In the first demonstration of the glymphatic system [6], the lowest molecular weight tracer Alexa 594 hydrazide (759 Da), with a molecular size approximately 2.5 times greater than that of oxycodone, rapidly disseminated throughout the brain after infusion into the cisterna magna [6]. That finding is in line with our present results, showing rather uniform distribution of oxycodone and naloxone across the brain interstitium.

While in the awake rats the naloxone C_{max} was reached already at the 30-min time point in several brain regions, treatment with dexmedetomidine increased both the C_{max} and T_{max}. This finding is in agreement with a rat magnetic resonance imaging (MRI) study, where dexmedetomidine supplementation also delayed the whole-brain T_{max} for the small-molecule MRI contrast agent gadopentetic acid (938 Da) [23]. We hypothesize that when the animals are awake, CSF is rapidly effluxed from the CNS via CSF exit routes such as nasal lymphatic vessels and very little enters the perivascular spaces and glymphatic pathway [7]. Dexmedetomidine, in contrast, may allow more CSF to reach the perivascular spaces of large arteries and carry dissolved drugs to the parenchyma.

This is the first study to test the effects of dexmedetomidine monotherapy on intrathecal delivery of clinically relevant drugs to the CNS. Stimulation of α_2-adrenergic autoreceptors by dexmedetomidine decreases the activity of locus coeruleus and norepinephrine release throughout the CNS [24,25], observed as sedation and increased slow-wave EEG oscillations [19], as in our study. In previous studies, ketamine-xylazine anesthesia that dramatically increases slow-wave oscillations enhanced the access of intracisternally-infused fluorescent CSF tracers to pial perivascular spaces [7] and brain parenchyma [15]. A recent study comparing six different anesthetic regimens highlighted a strong correlation between EEG delta power and CSF influx [16], and supplementing low-concentration isoflurane anesthesia with dexmedetomidine increased glymphatic transport compared with high-concentration isoflurane anesthesia alone [23]. The increase in glymphatic flow induced by NREM sleep-like states has been attributed to a decrease in astrocytic volume in the CNS parenchyma and a concomitant decrease in extracellular flow resistance due to higher interstitial volume [15]. Recently it was shown that cerebral arterial wall pulsatility induced by the cardiac cycle is the main driver of fluid in perivascular spaces of pial arteries [26]. Since dexmedetomidine may have cerebral vascular effects, further mechanistic studies are needed to assess the effects of dexmedetomidine on cerebral arterial wall pulsatility, periarterial size, and fluid flow. Taken together, there is increasing evidence that α_2-agonists could be useful in enhancing glymphatic flow and promoting drug delivery to the CNS.

In our study, morphine concentrations in the CNS were below the limit of quantification by our method, although naloxone and oxycodone could be reliably quantified. Morphine is a substrate of the drug efflux transporter P-glycoprotein [27,28] that is widely expressed not only at the BBB endothelium [29] but also at the arachnoid villus membranes [30], making morphine prone to efflux transport at several stages and possibly leading to very low CNS concentrations. Oxycodone shares many physicochemical properties with morphine and other water-soluble strong opioid analgesics [31]. However, in contrast to morphine, oxycodone has facilitated influx transport to the CNS at the BBB [32], which evidently predominates over efflux processes in our cisterna magna infusion model, whereas efflux must be the major factor in the case of morphine. Naloxone is a relatively lipid-soluble opioid antagonist with no known active transport at the BBB. In our study, despite a similar absolute dose of oxycodone and naloxone infused, we generally found higher naloxone than oxycodone concentrations in the CNS (Fig. 4), supposedly due to higher lipophilicity and increased intracellular penetration. The effect of dexmedetomidine on drug CNS delivery was slightly more pronounced in the case of oxycodone, probably because it is more prone to glymphatic fluxes due to its hydrophilicity. Further studies with a wider range of tracer molecules are needed to characterize the effects of CNS drug transporters and drug physicochemical properties on glymphatic CSF-ISF drug delivery.

The concentration of oxycodone in the spinal cord, the main target of opioids, was increased by 70% and 41% after systemic and intrathecal dexmedetomidine, respectively (Fig. 4B and S1B). In clinical anesthesia practice, intravenous and intrathecal α_2-agonists such as dexmedetomidine and clonidine have shown synergistic effects when combined with intrathecal opioids [33] and sodium channel blocker anesthetics such as bupivacaine and ropivacaine [34–39], leading to enhanced or prolonged analgesia. These beneficial effects have been explained by supposedly additive pharmacodynamic effects at the receptor level. Based on our findings, it is compelling to hypothesize that the beneficial effects of adjunct α_2-agonists may be in part due to a pharmacokinetic mechanism whereby dexmedetomidine leads to enhanced CSF-ISF fluid exchange and thus increased exposure. Indeed, our study raises a question whether other classes of intrathecal therapeutics such as antineoplastic compounds could be infused under dexmedetomidine sedation to enhance their glymphatic delivery to the CNS. Our proposal for a mechanism of action for dexmedetomidine in the enhanced delivery of intrathecally-administered small-molecule opioids is presented schematically in Fig. 5.

Dexmedetomidine is a relatively safe sedative agent that has been approved also for procedural sedation [17,18]. The main adverse effects are related to hemodynamic changes; at low plasma concentrations it reduces sympathetic outflow, often leading to hypotension [17]. However, higher concentrations may lead to transient hypertension due to the stimulation of vasopressor α_{2B}-adrenoreceptors [40], as seen in the present study and also in humans [41,42]. In our study, the 0.2 mg/kg dose was selected to produce hypnosis, immobility and loss of righting reflex for 2 h. The monitored plasma concentration was 8.8 ± 0.8 ng/mL (n = 4) at 60 min after administration. In humans, the therapeutic plasma concentration is 0.4–1.2 ng/mL for sedation and approximately 3.2 ng/mL for inducing loss of consciousness [42], however, concentrations as high as 14.7 ng/mL have been observed [43]. The concentrations used in humans for inducing loss of consciousness may be high enough to show enhancement of glymphatic flow and drug delivery.

An aspect that warrants further investigation concerns the pharmacokinetics after lumbar intrathecal administration, as opposed to the cisterna magna. The process may be slower in humans due to longer diffusion and influx distances. Indeed, a clinical study that assessed the kinetics of the magnetic contrast agent gadobutrol (605 Da) infused to the lumbar intrathecal space showed that the peak contrast enhancement in most of the studied deep cerebral areas occurred 24 h after tracer injection [44]. Enhancing drug exposure with procedural

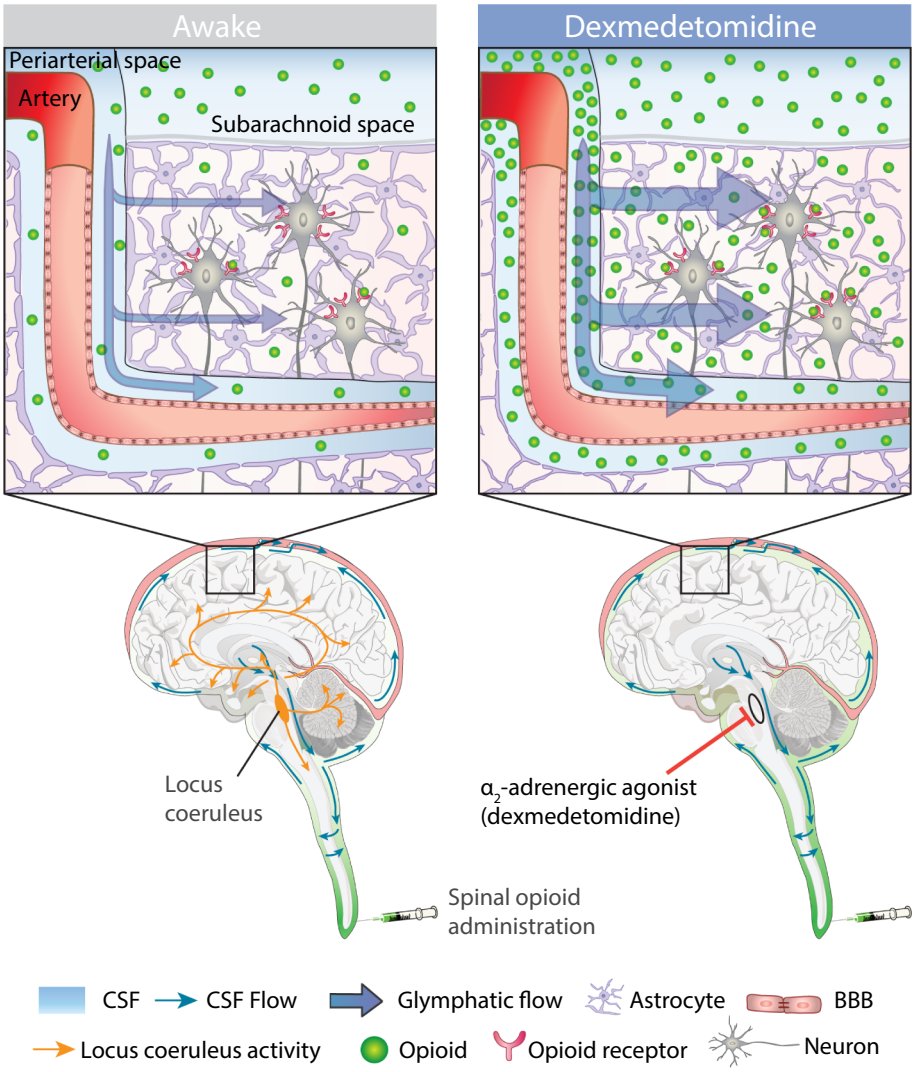

Fig. 5. Proposed mechanism of action for dexmedetomidine in the enhanced delivery of intrathecally-administered small-molecule drugs. In the awake state, the locus coeruleus is active, resuting in a high noradrenergic tonus throughout the neuraxis, and suppressed glymphatic activity. Dexmedetomidine reduces locus coeruleus firing rate via autoreceptor activation, leading to sedation with increased slow-wave EEG oscillations and an increased interstitial volume. Given the lower resistance to intestital bulk flow, there is enhanced glymphatic influx to the brain, which increases the delivery of small-molecule opioids from the subarachnoid space to the brain and spinal cord parenchymas. CSF, cerebrospinal fluid; BBB, blood-brain barrier.

dexmedetomidine sedation could have the greatest potential in delivering drugs that target the spinal cord near the site of infusion, such as the oligonucleotide nusinersen [3] used in the treatment of spinal muscular atrophy. The time needed to reach the target in spinal cord would likely be faster than in brain. Another non-pharmacological strategy to improve the glymphatic delivery of intrathecal therapeutics would be to administer them in the evening, i.e. before sleep. Due to daily clinical routines, most intrathecal infusions are administered during regular working hours, when the glymphatic pathway is disengaged.

5. Conclusions

Dexmedetomidine monotherapy increases the CNS delivery of intrathecally administered drugs in the rat brain and spinal cord by enhancing glymphatic transport. This phenomenon could potentially be utilized to enhance the delivery and efficacy of intrathecal therapeutics used in the treatment of CNS diseases. As sedation is frequently indicated for intrathecal drug delivery, clinical trials should be designed to study the effects of dexmedetomidine on drug delivery and response. Future studies with drugs with different physicochemical properties are needed to maximize the potential of the glymphatic system in drug delivery and to improve the safety and efficacy of intrathecally administered therapeutics.

Acknowledgements

We thank Jouko Laitila for expert assistance, Dan Xue for expert graphic illustrations, Anna L.R. Xavier for helpful discussions, and Terhi J. Lohela and Paul Cumming for comments on the manuscript.

Funding

This work was supported by Lundbeck Foundation, Novo Nordisk Foundation, Sigrid Jusélius Foundation, Finska Läkaresällskapet, University of Helsinki Research Funds, and European Union's Horizon 2020 research and innovation programme under the Marie Sklodowska-Curie grant agreement GlymPharma No 798944.

Author contributions

Tuomas O. Lilius: Conceptualization, Methodology, Validation, Formal Analysis, Investigation, Visualization, Writing – Original Draft, Project Administration, Resources, Funding Acquisition.
Kim Blomqvist: Investigation, Methodology, Validation.
Natalie L. Hauglund: Investigation, Methodology, Formal Analysis.
Guojun Liu: Investigation.
Frederik Filip Stæger: Formal Analysis, Visualization.
Simone Bærentzen: Investigation.
Ting Du: Investigation.

Fredrik Ahlström: Investigation.

Janne T. Backman: Methodology, Resources, Writing – Review & Editing.

Eija A. Kalso: Conceptualization, Resources, Writing – Review & Editing, Supervision, Funding Acquisition.

Pekka V. Rauhala: Conceptualization, Methodology, Resources, Investigation, Writing – Review & Editing, Supervision, Funding Acquisition.

Maiken Nedergaard: Conceptualization, Methodology, Resources, Writing – Review & Editing, Supervision, Funding Acquisition.

Competing interests

Eija A. Kalso is a member of advisory boards (Orion Pharma, Espoo, Finland, and Pierre Fabre, Toulouse, France). Other authors have no conflicts of interest to be reported.

Data availability

All data needed to evaluate the conclusions in the paper are present in the paper and/or the Supplementary Materials. Additional data related to this paper may be requested from the authors.

Appendix A. Supplementary data

Supplementary data to this article can be found online at https://doi.org/10.1016/j.jconrel.2019.05.005.

References

[1] P.S. Staats, T. Yearwood, S.G. Charapata, R.W. Presley, M.S. Wallace, M. Byas-Smith, et al., Intrathecal ziconotide in the treatment of refractory pain in patients with cancer or AIDS: a randomized controlled trial, Jama 291 (2004) 63–70, https://doi.org/10.1001/jama.291.1.63.

[2] A. Schulz, T. Ajayi, N. Specchio, E. de Los Reyes, P. Gissen, D. Ballon, et al., Study of intraventricular cerliponase alfa for CLN2 disease, N. Engl. J. Med. 378 (2018) 1898–1907, https://doi.org/10.1056/NEJMoa1712649.

[3] R.S. Finkel, E. Mercuri, B.T. Darras, A.M. Connolly, N.L. Kuntz, J. Kirschner, et al., Nusinersen versus sham control in infantile-onset spinal muscular atrophy, N. Engl. J. Med. 377 (2017) 1723–1732, https://doi.org/10.1056/NEJMoa1702752.

[4] D.J. Wolak, R.G. Thorne, Diffusion of macromolecules in the brain: implications for drug delivery, Mol. Pharm. 10 (2013) 1492–1504, https://doi.org/10.1021/mp300495e.

[5] M. Nedergaard, Neuroscience. Garbage truck of the brain, Science 340 (2013) 1529–1530, https://doi.org/10.1126/science.1240514.

[6] J.J. Iliff, M. Wang, Y. Liao, B.A. Plogg, W. Peng, G.A. Gundersen, et al., A paravascular pathway facilitates CSF flow through the brain parenchyma and the clearance of interstitial solutes, including amyloid β, Sci. Transl. Med. 4 (2012) 147ra111, https://doi.org/10.1126/scitranslmed.3003748.

[7] B.A. Plog, H. Mestre, G.E. Olveda, A.M. Sweeney, H.M. Kenney, A. Cove, et al., Transcranial optical imaging reveals a pathway for optimizing the delivery of immunotherapeutics to the brain, JCI Insight 3 (2018) 1188, https://doi.org/10.1172/jci.insight.120922.

[8] B.T. Kress, J.J. Iliff, M. Xia, M. Wang, H.S. Wei, D. Zeppenfeld, et al., Impairment of paravascular clearance pathways in the aging brain, Ann. Neurol. 76 (2014) 845–861, https://doi.org/10.1002/ana.24271.

[9] H. Mestre, L.M. Hablitz, A.L. Xavier, W. Feng, W. Zou, T. Pu, et al., Aquaporin-4-dependent glymphatic solute transport in the rodent brain, Elife 7 (2018) 74, https://doi.org/10.7554/eLife.40070.

[10] A. Aspelund, S. Antila, S.T. Proulx, T.V. Karlsen, S. Karaman, M. Detmar, et al., A dural lymphatic vascular system that drains brain interstitial fluid and macromolecules, J. Exp. Med. 212 (2015) 991–999, https://doi.org/10.1084/jem.20142290.

[11] A. Louveau, I. Smirnov, T.J. Keyes, J.D. Eccles, S.J. Rouhani, J.D. Peske, et al., Structural and functional features of central nervous system lymphatic vessels, Nature 523 (2015) 337–341, https://doi.org/10.1038/nature14432.

[12] J.J. Iliff, M.J. Chen, B.A. Plog, D.M. Zeppenfeld, M. Soltero, L. Yang, et al., Impairment of glymphatic pathway function promotes tau pathology after traumatic brain injury, J. Neurosci. 34 (2014) 16180–16193, https://doi.org/10.1523/JNEUROSCI.3020-14.2014.

[13] I. Lundgaard, M.L. Lu, E. Yang, W. Peng, H. Mestre, E. Hitomi, et al., Glymphatic clearance controls state-dependent changes in brain lactate concentration, J. Cereb. Blood Flow Metab. 37 (2016) 2112–2124, https://doi.org/10.1177/0271678X16661202.

[14] F. Wei, C. Zhang, R. Xue, L. Shan, S. Gong, G. Wang, et al., The pathway of subarachnoid CSF moving into the spinal parenchyma and the role of astrocytic aquaporin-4 in this process, Life Sci. (2017), https://doi.org/10.1016/j.lfs.2017.05.028.

[15] L. Xie, H. Kang, Q. Xu, M.J. Chen, Y. Liao, M. Thiyagarajan, et al., Sleep drives metabolite clearance from the adult brain, Science 342 (2013) 373–377, https://doi.org/10.1126/science.1241224.

[16] L.M. Hablitz, H.S. Vinitsky, Q. Sun, F.F. Stæger, B. Sigurdsson, K.N. Mortensen, et al., Increased glymphatic influx is correlated with high EEG delta power and low heart rate in mice under anesthesia, Sci. Adv. 5 (2019) eaav5447.

[17] M.A.S. Weerink, M.M.R.F. Struys, L.N. Hannivoort, C.R.M. Barends, A.R. Absalom, P. Colin, Clinical pharmacokinetics and pharmacodynamics of dexmedetomidine, Clin. Pharmacokinet. 56 (2017) 893–913, https://doi.org/10.1007/s40262-017-0507-7.

[18] C.R.M. Barends, A. Absalom, B. van Minnen, A. Vissink, A. Visser, Dexmedetomidine versus midazolam in procedural sedation. A systematic review of efficacy and safety, PLoS One 12 (2017) e0169525, , https://doi.org/10.1371/journal.pone.0169525.

[19] P.L. Purdon, A. Sampson, K.J. Pavone, E.N. Brown, Clinical electroencephalography for anesthesiologists: part I: background and basic signatures, Anesthesiology 123 (2015) 937–960, https://doi.org/10.1097/ALN.0000000000000841.

[20] A.L.R. Xavier, N.L. Hauglund, S. von Holstein-Rathlou, Q. Li, S. Sanggaard, N. Lou, et al., Cannula implantation into the cisterna magna of rodents, J. Vis. Exp. (2018) e57378, , https://doi.org/10.3791/57378.

[21] R. Moreno-Vicente, Z. Fernández-Nieva, A. Navarro, I. Gascón-Crespí, M. Farré-Albaladejo, M. Igartua, et al., Development and validation of a bioanalytical method for the simultaneous determination of heroin, its main metabolites, naloxone and naltrexone by LC-MS/MS in human plasma samples: application to a clinical trial of oral administration of a heroin/naloxone formulation, J. Pharm. Biomed. Anal. 114 (2015) 105–112, https://doi.org/10.1016/j.jpba.2015.04.044.

[22] B.B. Avants, N.J. Tustison, M. Stauffer, G. Song, B. Wu, J.C. Gee, The Insight ToolKit image registration framework, Front Neuroinform. 8 (2014) 44, https://doi.org/10.3389/fninf.2014.00044.

[23] H. Benveniste, H. Lee, F. Ding, Q. Sun, E. Al-Bizri, R. Makaryus, et al., Anesthesia with dexmedetomidine and low-dose isoflurane increases solute transport via the glymphatic pathway in rat brain when compared with high-dose isoflurane, Anesthesiology 127 (2017) 976–988, https://doi.org/10.1097/ALN.0000000000001888.

[24] C.M. Jorm, J.A. Stamford, Actions of the hypnotic anaesthetic, dexmedetomidine, on noradrenaline release and cell firing in rat locus coeruleus slices, Br. J. Anaesth. 71 (1993) 447–449.

[25] J.A. Ihalainen, H. Tanila, In vivo regulation of dopamine and noradrenaline release by alpha2A-adrenoceptors in the mouse prefrontal cortex, Eur. J. Neurosci. 15 (2002) 1789–1794.

[26] H. Mestre, J. Tithof, T. Du, W. Song, W. Peng, A.M. Sweeney, et al., Flow of cerebrospinal fluid is driven by arterial pulsations and is reduced in hypertension, Nat. Commun. 9 (2018) 4878, , https://doi.org/10.1038/s41467-018-07318-3.

[27] A.H. Schinkel, E. Wagenaar, L. van Deemter, C.A. Mol, P. Borst, Absence of the mdr1a P-Glycoprotein in mice affects tissue distribution and pharmacokinetics of dexamethasone, digoxin, and cyclosporin A, J. Clin. Invest. 96 (1995) 1698–1705, https://doi.org/10.1172/JCI118214.

[28] R. Xie, M. Hammarlund-Udenaes, A.G. de Boer, E.C. de Lange, The role of P-glycoprotein in blood-brain barrier transport of morphine: transcortical microdialysis studies in mdr1a (−/−) and mdr1a (+/+) mice, Br. J. Pharmacol. 128 (1999) 563–568, https://doi.org/10.1038/sj.bjp.0702804.

[29] A. Schinkel, P-Glycoprotein, a gatekeeper in the blood-brain barrier, Adv. Drug Deliv. Rev. 36 (1999) 179–194.

[30] Z. Zhang, M. Tachikawa, Y. Uchida, T. Terasaki, Drug clearance from cerebrospinal fluid mediated by organic anion transporters 1 (Slc22a6) and 3 (Slc22a8) at arachnoid membrane of rats, Mol. Pharm. 15 (2018) 911–922, https://doi.org/10.1021/acs.molpharmaceut.7b00852.

[31] R. Pöyhiä, T. Seppala, Liposolubility and protein binding of oxycodone in vitro, Pharmacol. Toxicol. 74 (1994) 23–27.

[32] E. Boström, M. Hammarlund-Udenaes, U.S.H. Simonsson, Blood-brain barrier transport helps to explain discrepancies in in vivo potency between oxycodone and morphine, Anesthesiology 108 (2008) 495–505, https://doi.org/10.1097/ALN.0b013e318164cf9e.

[33] E. Engelman, C. Marsala, Efficacy of adding clonidine to intrathecal morphine in acute postoperative pain: meta-analysis, Br. J. Anaesth. 110 (2013) 21–27, https://doi.org/10.1093/bja/aes344.

[34] X.-Y. Niu, X.-B. Ding, T. Guo, M.-H. Chen, S.-K. Fu, Q. Li, Effects of intravenous and intrathecal dexmedetomidine in spinal anesthesia: a meta-analysis, CNS Neurosci. Ther. 19 (11) (2013 Nov) 897–904, https://doi.org/10.1111/cns.12172 (Epub 2013 Oct 14).

[35] F.N. Kaya, B. Yavascaoglu, G. Turker, A. Yildirim, A. Gurbet, E.B. Mogol, et al., Intravenous dexmedetomidine, but not midazolam, prolongs bupivacaine spinal anesthesia, Can. J. Anesth. 57 (2010) 39–45, https://doi.org/10.1007/s12630-009-9231-6.

[36] V.S. Reddy, N.A. Shaik, B. Donthu, V.K. Reddy Sannala, V. Jangam, Intravenous dexmedetomidine versus clonidine for prolongation of bupivacaine spinal anesthesia and analgesia: a randomized double-blind study, J. Anaesthesiol. Clin. Pharmacol. 29 (2013) 342–347, https://doi.org/10.4103/0970-9185.117101.

[37] M.-H. Kim, S.Y. Jung, J.D. Shin, S.H. Lee, M.-Y. Park, K.M. Lee, et al., The comparison of the effects of intravenous ketamine or dexmedetomidine infusion on spinal block with bupivacaine, Korean J. Anesthesiol. 67 (2014) 85–89, https://doi.org/10.4097/kjae.2014.67.2.85.

[38] B.K. Rekhi, T. Kaur, D. Arora, P. Dugg, Comparison of intravenous dexmedetomidine with midazolam in prolonging spinal anaesthesia with ropivacaine, J. Clin.

Diagn. Res. 11 (2017) UC01–UC04, https://doi.org/10.7860/JCDR/2017/23874.9344.
[39] U.R. Kavya, S. Laxmi, V. Ramkumar, Effect of intravenous dexmedetomidine administered as bolus or as bolus-plus-infusion on subarachnoid anesthesia with hyperbaric bupivacaine, J. Anaesthesiol. Clin. Pharmacol. 34 (2018) 46–50, https://doi.org/10.4103/joacp.JOACP_132_16.
[40] N.L. Kanagy, Alpha(2)-adrenergic receptor signalling in hypertension, Clin. Sci. 109 (2005) 431–437, https://doi.org/10.1042/CS20050101.
[41] J. Penttilä, A. Helminen, M. Anttila, S. Hinkka, H. Scheinin, Cardiovascular and parasympathetic effects of dexmedetomidine in healthy subjects, Can. J. Physiol. Pharmacol. 82 (2004) 359–362, https://doi.org/10.1139/y04-028.
[42] A. Snapir, J. Posti, E. Kentala, J. Koskenvuo, J. Sundell, H. Tuunanen, et al., Effects of low and high plasma concentrations of dexmedetomidine on myocardial perfusion and cardiac function in healthy male subjects, Anesthesiology 105 (2006) 902–910 (quiz 1069–70).
[43] T.J. Ebert, J.E. Hall, J.A. Barney, T.D. Uhrich, M.D. Colinco, The effects of increasing plasma concentrations of dexmedetomidine in humans, Anesthesiology 93 (2000) 382–394.
[44] G. Ringstad, L.M. Valnes, A.M. Dale, A.H. Pripp, S.-A.S. Vatnehol, K.E. Emblem, et al., Brain-wide glymphatic enhancement and clearance in humans assessed with MRI, JCI Insight 3 (2018), https://doi.org/10.1172/jci.insight.121537.